Published in final edited form as:
J Neurobiol. 2003 March ; 54(4): 539–554. doi:10.1002/neu.10192.

Vitamin A Deficiency Leads to Increased Cell Proliferation in Olfactory Epithelium of Mature Rats

M. A. Asson-Batres[1], **M.-S. Zeng**[1], **V. Savchenko**[2], **A. Aderoju**[1], and **J. McKanna**[2]

[1]Department of Biological Sciences, Tennessee State University, P.O. Box 1116, 3500 John A. Merritt Blvd., Nashville, Tennessee 37209

[2]Department of Cell Biology, Vanderbilt University, Nashville, Tennessee

Abstract

We have shown previously that vitamin A deficiency (VAD) leads to the decreased expression of gene products that are specifically synthesized by mature neurons in the olfactory epithelium (OE) of adult rats. These results support the hypothesis that retinoic acid, a derivative of vitamin A, is required for neurogenesis and neuron replacement *in vivo*. VAD does not cause gross degeneration of the OE, raising the question: what types of cells continue to populate VAD OE? In this study, we compared the cell densities of VAD and VA-sufficient (VAS) OE and investigated whether cell proliferation is upregulated in VAD OE. The results show that (1) total cell number in VAD and VAS OE are comparable; (2) localized areas of hyperplasia are present in the basal regions of VAD, but not VAS, OE; (3) there is a substantial increase in the number of PCNA (proliferating cell nuclear antigen) positive cells in the basal region of VAD OE relative to VAS OE; and (4) there is a relative increase in the levels of mRNA encoding the transcription factor, MASH I, in VAD OE. We conclude that reduced availability of vitamin A derivatives, such as retinoic acid, leads to a loss of control over proliferation, hyperplasia, and increased numbers of pro-neural cells *in vivo*.

Keywords

vitamin A; retinoic acid; neurogenesis; olfactory epithelium; neuron

INTRODUCTION

Neurons in the olfactory epithelium of postnatal mammals die, presumably in response to environmental insults or terminal differentiation (Magrassi and Graziadei, 1995; Murray and Calof, 1999), and are replaced throughout life (Graziadei and Graziadei, 1979). The process involves proliferation of progenitor cells thought to reside in the basal layer of the epithelium and progressive differentiation of the progeny cells into postmitotic populations of functionally immature and mature neurons (Calof and Chikaraishi, 1989; Verhaagen et al., 1989; Schwob et al., 1995; Mackay-Sim and Chuah, 2000). The factors that participate in this process and the mechanisms that direct it are not fully understood.

all-trans-Retinoic acid is an oxidized derivative of vitamin A (*all-trans*-retinol) that has been implicated in neurogenesis. An involvement of retinoic acid in this process has been suggested by: (1) *in vitro* studies where addition of retinoic acid to cell culture medium has

Correspondence to: M.-A. Asson-Batres (massonbatres@tnstate.edu).

been shown to induce the differentiation of stem cells into cells with neuronal characteristics (Balboni et al., 1991; Kelley et al., 1994; Bain et al., 1996); (2) whole animal studies where injection of retinoic acid into the circulation has been shown to induce the development of neurons (Kelley et al., 1999); and (3) whole animal genetic, nutritional deficiency, and enzyme localization studies that support the idea that availability of retinoic acid affects the development of neuronal pathways during embryogenesis (LaMantia et al., 1993; Anchan et al., 1997; Dickman et al., 1997; Drager et al., 1998; Niederreither et al., 2000; White et al., 2000; Hoover et al., 2001; Smith et al., 2001). Recently, our laboratory has demonstrated that retinoic acid levels are depleted in the olfactory tissue of postnatal rats that have been nutritionally deprived of vitamin A. We have observed that this deficiency of retinoic acid in olfactory tissue is accompanied by a decrease in the expression of proteins (and the mRNAs that encode them) that are specifically found in mature olfactory neurons. The results suggest that there is a loss of mature neurons in vitamin A deficient (VAD) olfactory epithelium (OE) and provide support for the notion that retinoic acid affects neurogenesis *in vivo*.

If mature neurons are lost and not replaced in VAD OE, one would expect the tissue to eventually lose its integrity and structural organization. At a superficial level, however, the OE of VAD rats looks normal. That is, the tissue of VAD rats is intact and has the same general morphologic organization and apparent cell density as does tissue found in vitamin A-sufficient (VAS) animals. This suggests there may be compensatory increases in the numbers of other OE cell types that serve to fill the void created by VAD-imposed loss of mature neurons from the tissue. There are four main types of cells in the OE: basal cells (globose and horizontal), immature neurons, mature neurons, and sustentacular (glial-like) cells. Globose basal cells are thought to proliferate, differentiate, and give rise to immature neurons, which in turn, differentiate into mature neurons. One possibility that may explain the apparent similarity in cell density of VAD and VAS OE is that retinoic acid may be required to signal cells to progress through the neuron differentiation process. In the absence of retinoic acid, cell proliferation may increase, and a population of developmentally arrested, neural progenitor cells may build up in the mature neuron-deficient OE.

In this study, we confirmed that cell densities are similar in VAD and VAS OE, and determined that cell proliferation is increased over control levels in VAD OE. We determined further, that expression of the mammalian achaetescute homolog (MASH I) mRNA is increased in olfactory tissue from VAD rats. We suggest that VAD may lead to a block in the neuron differentiation pathway at a step involving MASH I-positive pro-neural basal cells.

MATERIALS AND METHODS

Vitamin A Deprivation

Male, Long-Evans rats (Harlan-Sprague-Dawley, Maximum-barrier-maintained/viral-antibody-free, outbred colony), 21 days of age, weighing approximately 35– 40 g were individually housed in wire mesh-bottom cages, without bedding, in animal care facilities at Vanderbilt University. All guidelines stipulated in *The Guide for Care and Use of Laboratory Animals*, National Academic Press were met. The animals were fed regular rat chow (diet contains a source of vitamin A) for 1 week. The animals were then randomly assigned to two groups. Dietary vitamin A deficiency was induced by feeding one group of rats a purified, retinoid-free, custom diet (# 904646, ICN Biochemicals Inc., Aurora, OH) (experimental, VAD group). The second group of rats was fed the same diet as the experimental group, but supplemented with 8 mg gelatin-stabilized, retinyl palmitate per kg of diet (control, VAS group). Experimental animals were fed *ad libitum* and control animals

were fed an amount equal to the average daily consumption of the experimental animal group.

Data from a separate group of rats (followed during the same study and fed the diet for a similar period of time) indicated that both retinoic acid and retinol are depleted in olfactory mucosa from VAD rats (to be published elsewhere). The retinoid status of olfactory tissue used for histochemistry and RNA isolation could not be measured. Thus, we relied on the comparative daily weight gain of rats as one indicator of VA status in these animals (Smith, 1990). Other indicators were white lower incisors, alopecia, and/or ataxia. When experimental animals attained a weight that was 20 –30% less than their peak weight and displayed at least one further indicator of VAD, they were sacrificed. Nine VAS and nine VAD rats were used for this study. Three VAS (N2, N3, and N4) and three VAD (D5, D14, and D24) rats were used for immunohistochemistry and *in situ* hybridization studies. The remaining six VAS rats (N7, N8, N19, N21, N26, and N38) and six VAD rats (D8, D28, D34, D36, D37, and D39) were used to prepare individual samples of total RNA. A summary of the characteristics of rats maintained on the VAS and VAD diets is presented in Table I.

Tissue Preparation for Histochemical Analyses

Animals were anesthetized with 70 mg/kg ketamine/14 mg/kg xylazine/7 mg/kg acetopromazine, perfused transcardially with heparinized saline, followed by Perfix (4% para-formaldehyde/20% isopropanol/2% trichloroacetic acid/2% zinc chloride), and postfixed overnight with the same fixative. For preparations of *regio olfactoria*, skulls were de-calcified in 3% formic acid for 3 days and trimmed according to the protocol of Young (1981). Coronal sections of *regio olfactoria* from the most posterior region of the nasal cavity were used in this study. Tissues were dehydrated in graded ethanol/xylene and embedded in paraffin. Paraffin sections (5 μm) were cut by staff in the Vanderbilt University Histopathology Laboratory (Nashville, TN) using RNAse-free conditions. The sections were collected on poly-l-lysine– coated microscope slides and stored until use at 4°C (for immunohistochemistry studies) and at −20°C (for *in situ* hybridization studies).

Light Microscopic Immunocytochemistry

Regio olfactoria tissue sections from three VAS and three VAD rats were rehydrated with phosphate-buffered saline (PBS). Antigen retrieval was carried out using target retrieval solution according to the manufacturer's protocol (DAKO Corporation, Carpenteria, CA). Nonspecific binding was blocked by incubation in 10% normal goat serum for 1 h. Sections were incubated with a 1:300 dilution of Anti-Proliferating Cell Nuclear Antigen (PCNA) monoclonal mouse antibody (#M0879, DAKO) in 1% normal goat serum at 4°C overnight, followed by incubation with a biotin-labeled secondary antibody (# 115-065-100, Jackson ImmunoResearch Laboratories, West Grove, PA), and then by incubation with a horseradish peroxidase-conjugated antibiotin tertiary antibody (# 200-032-096, Jackson ImmunoResearch Laboratories). After washing with PBS, the sections were processed for peroxidase activity using diaminobenzidine (DAB) and peroxide as substrates.

Cell Counts

Regio olfactoria tissue sections from two VAS and two VAD rats were stained with toluidine blue, and the total number of nuclei in the olfactory epithelium lining one side of the nasal septum of each section were counted. A BIO-QUANT computerized image analysis system (R&M Biometrics, Inc., Nashville, TN) was used to map the tissue sections, measure tissue dimensions, and tally the number of nuclei. Color video images were obtained with the measuring system (Leitz Orthoplan microscope, Optronics 3-chip color camera, BIOQUANT BQ-4000 frame grabber). In initial automated steps of the image

analysis, digital color thresholds distinguished the blue density objects in the images and size filters. Epithelial width and numbers of nuclei were determined for contiguous 143 μm long segments of olfactory epithelium lining the nasal septum. The total number of nuclei in each 143 μm segment was plotted versus the width of the epithelium. The data were analyzed for goodness of fit using least squares linear regression.

$PCNA^+$ cell profiles were counted along the basal lamina of the OE lining the turbinates and nasal septum of one-half of a coronal tissue section from each of three VAS and three VAD animals. Epithelium length was measured, and cell densities were expressed as number of $PCNA^+$ cell profiles per mm OE.

In Situ Hybridization

A cDNA fragment encoding olfactory marker protein (OMP), a specific marker of mature olfactory neurons, was generated using RT-PCR. Oligonucleotide primers were designed using the rat OMP cDNA sequence (NIH Gene-Bank Accession # NM_012616). The PCR product was subcloned into PCR-Script (Stratagene Cloning Systems, La Jolla, CA), and sequenced in both directions for verification. Sense and antisense riboprobes labeled with digoxigenin-UTP (Roche Diagnostics Corp., Indianapolis, IN) were synthesized using a Riboprobe *in vitro* transcription kit (Promega, Madison, WI). *Regio olfactoria* tissue sections from three VAS and three VAD rats were deparaffinized and rehydrated in water, digested with proteinase K, dehydrated in alcohol, preincubated with hybridization solution (# H7782, Sigma Chemicals, St. Louis, MO) at 42°C for 10 min, and then incubated with 450 ng/mL probe in hybridization solution at 42°C overnight. The sections were washed in 2× SSPE (0.02 *M* NaH_2PO_4/2 m*M* EDTA/0.3 *M* NaCl) at room temperature for 5 min × 2, and then in 0.2× SSPE at 55°C for 20 min × 2, treated with 5 μg/mL RNAse at 37°C for 30 min, and washed again in 0.2× SSPE at 55°C for 20 min × 2. A DIG Nucleic Acid Detection Kit (#1175041, Roche Diagnostics Corp.) was used to detect hybridized riboprobes. Color development was with nitroblue tetrazolium according to the manufacturer's protocol.

Quantitative RT-PCR

Tissue Dissection and Storage—Rats were euthanized with an overdose of carbon dioxide. The head was removed, skinned, and put on ice. Olfactory tissue lying beneath the nasal bone and lining the nasal septum and turbinates was dissected and transferred to RNA Later™ (Ambion Inc., Austin, TX) to prevent RNA degradation, using the tissue weight/volume ratio recommended by the manufacturer. Tissue was stored at −20°C until RNA isolation.

Total RNA Isolation—Total RNA was isolated from olfactory tissue from each of six VAS and six VAD rats following the guanidine isothiocyanate (GITC)-cesium chloride gradient centrifugation method of (Wilkinson, 1991) with the following modifications. Tissues were brought to room temperature and examined to ensure that crystalline deposits of RNA Later™ were completely in solution. The RNA Later™ was removed with a clean plastic pasteur pipet. The tissue was homogenized in a 10-fold volume of GITC (4 *M* guanidine isothiocyanate/0.7% β-mercaptoethanol) using a Tektron homogenizer for four 15-s bursts at full speed. To shear genomic DNA, the homogenate was passed through an18-gauge needle once, and then through a 22-gauge needle twice. The homogenate was collected in a sterile 25-mL plastic, conical centrifuge tube, and 3 mL was carefully overlaid on 1.8-mL 4M cesium chloride in a 5 mL polyal-lomer centrifuge tube, and centrifuged in a swinging bucket rotor at 30,000 × *g* at 18°C for 12–18 h in a Beckman LC-300 ultracentrifuge. Following centrifugation, the RNA pellet was resuspended in water and extracted twice with phenol/chloroform and twice with butanol/chloroform, followed by

precipitation of the RNA with ethanol. The pellet was resuspended in RNAse-free water and stored at −70°C until use.

DNAse Treatment—The RNA samples were reacted with DNase I (DNA-*free*™, Ambion, Inc.) according to the manufacturer's directions. The DNA-free RNA was precipitated using QuikPrecip™ (Edge Biosystems, Gaithersburg, MD) according to the manufacturer's directions, and the pelleted RNA was resuspended in RNase-free water.

Quantification and Analyis of RNA—An amount of 0.5 μL of the resuspended RNA sample was added to 50 μL RNase-free water, transferred to a 50 μL spectrophotometer cell (1-cm path length), and the concentration determined by reading the absorbance at 260 nm (1 OD_{260} = 40 μg/mL). The equivalence of RNA concentrations in samples from different animals was verified by separating 0.5 μg of each RNA sample on a 1.0% native agarose gel/1× TBE (pH 7.8) at 70 V, staining the RNA with ethidium bromide, and comparing the intensities of the 18S and 28S ribosomal RNA (rRNA) bands using a BIO-RAD Gel-Doc 1000 Imaging System and Quantity One image analysis software (BIO-RAD, Hercules, CA). The quality of the RNA was assessed by analyzing the 28S:18S rRNA ratios, and by visually assessing the gels for the presence of DNA and/or signs of degraded RNA.

cDNA First-Strand Synthesis—cDNA was synthesized from the VAS and VAD RNA samples using 1 μg DNA-free, total RNA and random hexamers in a 20 μL reaction catalyzed by SuperScript™ II RNAse H^- reverse transcriptase according to the manufacturer's protocol (Invitrogen, Baltimore, MD).

Initial Experiments to Confirm the Accuracy and Reproducibility of the Method of Quantitation—To test for variation in product yield in different reaction tubes due to the method of preparation or well-to-well differences in the thermocycler, 24 identical 100-μL PCR were prepared using cDNA prepared from olfactory tissue (as described above) and primers known to produce a single 300-bp gene fragment (see below for PCR protocol). Equal volumes (10 μL) of the reaction products were separated on agarose gels and stained with SYBR Gold (Molecular Probes, Eugene, OR). The intensity of the product in each lane was determined using the image analysis system described above.

An experiment was conducted to assess the accuracy of the method of quantitation. The remaining PCR samples were pooled, and the DNA concentration was determined by spectrophotometry (1 OD_{260} = 50 μg/mL). Serial dilutions of the samples were made and increasing amounts of DNA were separated on agarose gels and stained with SYBR Gold (Molecular Probes). Three separate gels were prepared. The intensities of the bands in each lane were determined, and the combined data from all gels (experiments 1, 2, and 3) were simultaneously plotted versus the amount of DNA loaded in the lane. The best fit curve was determined using least squares linear regression.

Product Yield Curves—Product yield profiles were determined for an internal control gene (18S rRNA) and for MASH I using one VAS (control) cDNA sample. Primers for 18S rRNA were from Ambion, Inc. These primers produce a 488 bp PCR product. Primers for MASH I were designed based on the rat MASH I sequence (NIH Gene-Bank Accession # X53725) and synthesized by BioSource International, Foster City, CA. The upstream primer was 5′-GGCTCAACTTCAGTGGCTTC-3′, and the downstream primer was 5′-TGGAGTAGTTGGGGGAGATG-3′. These primers produce a 291-bp PCR product. Reactions were prepared in HotStart tubes (Molecular Bio-Products, Inc., San Diego, CA), and contained 1 μL cDNA/1.5 m*M* $MgCl_2$/200 n*M* primers/0.2 μM dNTPs/2.5 U/μL TAQ polymerase in PCR buffer (Promega) in a final volume of 100 μL. The reactions were preincubated at 94°C for 2 min, and then incubated at 94°C × 1 min, 55°C × 1 min, 72°C ×

1.5 min for varying numbers of cycles in a Perkin-Elmer 2400 thermocycler. Aliquots of the 18S rRNA and MASH I reaction mixes were removed after increasing numbers of cycles of amplification (cycles 13–20 for 18S rRNA; cycles 31–39 for MASH I), incubated at 72°C for an additional 10 min, and placed on ice. Equal volumes of the products were separated on 0.8% agarose/TBE gels and stained with SYBR green I (Molecular Probes). Band intensities were determined using an image analysis system, as described above. Relative intensities of the products were plotted versus cycles of amplification to generate the product yield profiles.

Comparison of the Expression Levels of 18S rRNA and MASH I in VAS and VAD Animals—Independent RT-PCR reactions were prepared with RNA from six VAS and six VAD animals. One set of reactions contained primers specific for 18S rRNA and another set contained primers specific for MASH I. To quantify differences observed in product yield, the band intensities of gel-separated VAS (control) RT-PCR samples were averaged, and the band intensities of each gel-separated VAD sample was expressed as a percent of the control average. The statistical significance of band intensity differences was evaluated using a Mann-Whitney Rank Sum Test. Each experiment was carried out two times.

Photography

Photographic slides were taken with a Nikon FE 35 mm camera attached to a Nikon TE 300 inverted microscope. The 35-mm slides were digitized using a Polaroid Sprint-Scan system, and the images were edited and formatted using Adobe Photoshop computer software.

RESULTS

Vitamin A Deficiency

The rats used in this study were 27 days old when the study began, and they were maintained on the vitamin A-deficient and control diets for 135–158 days. Due to the number of rats in the study and the length of time it takes to sacrifice, fix, and prepare the tissues for storage, not all animals could be sacrificed on the same day. Additionally, not all rats developed indicators of the deficiency in the same amount of time. This was likely due to differences in the levels of their vitamin A stores at the time they entered the study and also due to physiological differences in their metabolism of vitamin A. Thus, a set of parameters defining equivalent states of deficiency was defined (as described in Materials and Methods, above), and the rats were sacrificed when they expressed these characteristics (Table I).

The rate of weight gain was equivalent for VAD and VAS rats for approximately 100 days. The animals in both groups gained approximately 5 g per animal per day until day 50 of the diet, and then the growth rate slowed to 2 g per animal per day or less. Beginning on day 100 of the diet, the VAD animals began to decrease in weight. On day 100, the VAD rats weighed 4% less on average than the VAS rats, whereas on the day of sacrifice, the VAD rats weighed 23% less on average than the VAS rats. The general health of the VAD animals was good on the day of sacrifice, although they exhibited known signs of the deficiency, including a loss of weight, white teeth, alopecia, ataxia, wheezing, and reddened eyes.

Visible Differences in the Cellular Morphology of VAD and VAS OE

The OE is a pseudostratified epithelium composed of four major cell types that can be distinguished by molecular markers. Basal cells (which include neuron progenitor cells) lie along and just above the basal lamina (bl, Fig. 1). Functionally immature neuron cell bodies (which can be distinguished by their expression of GAP-43, but not olfactory marker

protein, OMP) are located in layers just above the basal cell layer, and functionally mature neuron cell bodies (which are OMP^+ and GAP-43^-) are centrally located in layers just above the GAP-43^+ cell bodies (mn, Fig. 1). Sustentacular cell bodies form a single layer in the apical region of the OE just above the mature neurons (s, Fig. 1). The *lamina propria* (lp, Fig. 1) underlies the basal lamina and is composed of extracellular matrix material, fibroblasts, capillaries, Bowman's glands, and nerve fascicles.

VAD does not cause gross degeneration of mature rat OE. As shown in Figure 1(B) and (D), the VAD tissue is intact, and toluidine blue-stained nuclei are present throughout all layers of the VAD OE.

On closer inspection, we observed differences in the morphology of VAS and VAD OE. Note there are more nuclei in the basal regions of VAD OE than there are in the basal regions of VAS OE [compare regions designated by arrows in the VAD images, Fig. 1(B) and (D) with those in the VAS images, Fig. 1(A) and (C)]. The nuclei in the basal region of VAD OE are also larger, rounder, and more punctate in appearance than are the nuclei in VAS OE. Many, but not all, regions of VAD OE lining the septum and turbinates of *regio olfactoria* sections [Fig. 2(A)] showed this prominent increase in cell densities in the basal regions of the VAD tissue. In comparison, no regions of VAS OE displayed these notable differences in cell density, distribution, or appearance.

Total Cell Number Is Similar in VAD and VAS OE

Computer-generated maps of coronal sections of VAD and VAS *regio olfactoria* sections were produced using a BIOQUANT software image analysis program. An example of the image map generated from one tissue section is shown in Figure 2(A). We noted that the overall topography of the mature rat OE was not affected by VAD (data not shown). In general, the width of the OE was similar in VAS and VAD tissues, with the distance from the basal lamina to the apical edge of the OE ranging from 40 –90 μm.

The total number of toluidine blue-stained nuclei in the OE lining one side of the nasal septum [s, Fig. 2(A)] of each of two VAS rats and two VAD rats was determined. The OE lining the nasal septum was chosen for analysis because this region showed the least amount of topologic variation between rats. Total cell number per given area of OE varied from animal to animal for both VAS and VAD rats [compare VAS rats N3 and N4 in Fig. 2(B) and VAD rats D5 and D24 in Fig. 2(C)]. As indicated by least-squares linear regression analysis, there was a positive correlation between OE width and total cell number in a 143 μm length of OE for VAS animal N3 [Fig. 2(B), $r^2 = 0.59$], VAS animal N4 [Fig. 2(B), $r^2 = 0.73$], and VAD animal D24 [Fig. 2(C), $r^2 = 0.58$]. For these animals, the number of cells in an equivalent area of OE was generally comparable [100 to 200 cells in OE 143 μm in length × 50 μm in width, and 150 –250 cells in OE 143 μm in length × 80 μm in width, Fig. 2(B) and (C)]. The data were not correlated for VAD animal D5 [Fig. 2(C), $r^2 = 0.25$]. This was due to the presence of exceedingly high numbers of cells in the basal region of some areas of the nasal epithelium of this animal (similar to the regions shown in Fig. 1(B) and (D)].

Expression of PCNA Protein Islincreased in the OE of Mature VAD Rats

Figure 3 depicts results obtained when *regio olfactoria* sections from three different VAS and three different VAD rats were reacted with either an antisense riboprobe directed against olfactory marker protein (OMP) mRNA [Fig. 3(A)–(F)] and or an antibody directed against proliferating cell nuclear antigen [PCNA; Fig. 3(G)–(L)]. OMP is a gene product that is specifically expressed by mature olfactory neurons, and PCNA is an indicator of cells in the S phase of mitosis.

The antisense OMP riboprobe hybridized with cell bodies in the midregion of VAS and VAD OE. There was abundant expression of OMP mRNA in VAS OE [Fig. 3(A), rat N2; Fig. 3(B), rat N3; and Fig. 3(C), rat N4], but relatively little expression of this mature neuron marker in VAD OE [Fig. 3(D), rat D5; Fig. 3(E), rat D14; and Fig. 3(F), rat D24]. Staining was consistent throughout the *regio olfactoria* sections for VAS animals N3 and N4 and VAD animals D14 and D24, but was discontinuous and variable for VAS animal N2 and VAD animal D5 (data not shown). Control sections from the 3 VAS and 3 VAD animals showed little or no staining with the sense probe.

The anti-PCNA antibody labeled cell bodies in the basal regions of VAS and VAD OE in *regio olfactoria* sections [Fig. 3(G)–(L)]. Negative controls, in which the primary antibody was omitted from the experiment, showed no staining on either VAS or VAD tissue sections.

PCNA-positive cells were discontinuously dispersed along the basal lamina throughout all areas of VAS *regio olfactoria* sections [Fig. 3(G), rat N2; Fig. 3(H), rat N3; and Fig. 3(I), rat N4] and VAD *regio olfactoria* sections [Figs. 3(J), rat D5; Fig. 3(K), rat D14; and Fig. 3(L), rat D24]. The number of reactive cells was greater in some areas of both VAS and VAD tissues than in others. Reactive nuclei were mainly located in the basal region of VAS and VAD OE, although a few outliers were observed in the middle and more apical regions of the OE. Weak staining of nuclei was observed in sustentacular cell nuclei in some areas of sections from animals N3 and N4 (data not shown).

As indicated by reactivity of the PCNA antibody with VAD and VAS tissue sections, there were many more proliferative cells in the basal region of VAD OE than there were in VAS OE [compare the results in Fig. 3(J), (K), and (L) with those in Fig. 3(G), (H), and (I)]. Certain areas of the section from animal D5 [Fig. 3(J)] had exceedingly large clusters of PCNA-positive cells in the basal region of the OE. These localized areas of hyperplasia were complementary to areas showing high cell densities in the toluidine blue-stained tissue section from this animal [see Fig. 1(B) and Fig. 2(C), curve VAD D5, above].

$PCNA^+$ cell profiles were counted in the OE of VAS rats N2 (162 days of age), N3 (185 days of age), and N4 (185 days of age) and in the OE of VAD rats D5 (182 days of age), D14 (182 days of age), and D24 OE (178 days of age). There were 5, 13, and 9 $PCNA^+$ cell profiles/mm OE in the tissue sections from VAS rats N2, N3, and N4, respectively. There were 68, 29, and 34 $PCNA^+$ cell profiles/mm OE in the tissue sections from VAD rats D5, D14, and D24, respectively.

Expression of MASH I mRNA Is Increased in Mature VAD Rat Olfactory Tissue

It has been shown that changes in gene expression levels can be quantified by reverse transcriptase polymerase chain reaction (RT-PCR) (Wang et al., 1989). We evaluated various protocols for RT-PCR and determined that, to obtain reliable and reproducible results, it is necessary to (1) establish that equal amounts of high quality, DNA-free RNA are used to prepare RT-PCR samples; (2) establish comparable amplification conditions for all samples; (3) validate the method of quantitation; and (4) determine the linear range of amplification for each gene of interest for one control sample to select the number of cycles of amplification for the actual experiment. We have also determined that coamplification of two target genes in the same reaction mix adversely affects the reproducibility of the results, and thus, the accuracy of the method. Even when competimers are included in the reaction mix to balance product yields from different genes, we find the reaction kinetics are too complex to ensure reproducibility of results. We have found we obtain the most reliable results when we establish comparable reaction conditions for all of the genes of interest

(with the exception of the number of cycles of amplification) and then run the reactions independently of one another.

Equal Amounts of High Quality, DNA-free RNA Used to Prepare RT-PCR Samples—As can be seen in Figure 4(A), the RNA used in the experiments was of very good quality. A DNA-containing band is visible in the lane containing liver RNA that was not treated with DNase [LIV, lane 1, Fig. 4(A)]. It appears that DNase I treatment removed DNA from all but one of the other RNA samples shown in Figure 1(A) (VAD sample D8). The average ratio of the 28S:18S rRNA band intensities was 2.0 for the VAS RNA samples [N8, N19, N21, N26, and N38, Fig. 4(A)]. The average ratio of the 28S:18S rRNA band intensities was 2.5 for the VAD RNA samples [D8, D28, D34, D36, D37, and D39, Fig. 4(A)]. There was no sign of degradation of RNA in any of the lanes on the gel. Because it appeared that VAD sample D8 had residual DNA in the sample, it was not included in any further analyses. VAS sample N7 [not shown in Fig. 4(A)] was also excluded from further analyses to maintain equal VAS and VAD sample size.

Visual inspection of the gel and comparison of the 18S rRNA band intensities indicated that the VAS and VAD olfactory tissue RNA samples contained equivalent amounts of RNA. The average band intensities of the VAS and VAD 18S rRNA bands were within 5% of one another [Fig. 4(A), VAS sample band intensities, mean ± S.D. = 1179 ± 48; VAD sample band intensities, mean ± S.D. = 238 ± 37]. The intensities of the 28S rRNA bands were slightly higher in the VAD samples than in the VAS samples (VAD sample band intensities, mean ± S.D. = 3033 ± 595; VAS sample band intensities, mean ± S.D. = 2382 ± 145). Whether this elevation in 28S rRNA expression is biologically relevant is not known.

Comparable Amplification Conditions for All Samples and Validation of the Method of Quantitation—The same PCR was prepared in 24 different tubes and amplified in the 24 wells of a thermocycler. The intensities of the gel-isolated, PCR products from the 24 reactions were not significantly different from each other [Fig. 4(B)]. The percent difference in the measured intensities of equivalent volumes of the samples was 18% [samples 1– 8, gel one, Fig. 4(B)], 20% [samples 9 –16, gel two, Fig. 4(B)], and 21% [samples 17–24, gel three, Fig. 4(B); where percent difference = difference between minimum and maximum intensities/mean of minimum and maximum intensities].

We determined that band intensity (over the range used in the experiments reported here) showed a strong positive correlation with the amount of DNA separated on the gel [Fig. 4(C)].

Linear Range of Amplification for the Genes of Interest—We determined the product yield profiles for 18S rRNA and MASH I in one control (VAS) olfactory RNA sample. The product yield profiles for both gene products were sigmoidal in shape, but displaced from one another due to differences in the starting amounts of gene-specific cDNA [Fig. 4(D) and (E)]. 18S rRNA is a very abundant gene product and is detected after 13 cycles of amplification [Fig. 4(D), upper panel]; MASH I is a low abundance gene product in olfactory tissue and is detected after 30 cycles of amplification [Fig. 4(D), lower panel].

Effect of VAD on the 18S rRNA Product Yield Curves—Because cell densities are comparable in VAS and VAD OE (see Total cell number is similar in VAD and VAS OE, above), and there is no apparent effect of VAD on 18S rRNA levels [Fig. 4(A)], one would expect that the levels of cDNA encoding 18S rRNA amplified in RT-PCR would be similar in the VAS and VAD samples. We predicted that if the levels of expression for a particular gene were the same in the samples under comparison, that amplification of the samples

using gene-specific primers should yield overlapping product yield profiles, whereas if differences existed in the relative levels of gene expression in the control and experimental samples, one would obtain product yield curves that would be offset, indicating different starting levels of mRNA in the two populations. To verify this prediction, we compared the RT-PCR product yield curves for 18S rRNA in one VAD and one VAS olfactory RNA sample. VAD did not affect the expression of 18S rRNA, as is indicated by the overlapping product yield profiles of 18S rRNA amplified from VAS sample N4 and VAD sample D5 [Fig. 4(E)]. This result demonstrates, further, that 18S rRNA is an appropriate internal control gene for these experiments.

Effect of VAD on MASH I Product Yield Curves—VAD affected the expression of MASH I mRNA levels as is indicated by the leftward shift of the product yield curve for VAD sample D5 relative to that of VAS sample N4 [Fig. 4(E)]. The latter result indicates that the starting amount of MASH I mRNA in the VAD RT-PCR was greater than it was in the VAS sample.

Selection of the Number of Cycles of Amplification to Use for Quantitative RT-PCR—We used the product yield curves [Fig. 4(D)] to select the number of cycles to use for subsequent single-point, quantitative RT-PCR. We chose the number of cycles that produced an amount of product whose band intensity lied at the lower end of the linear range of the product yield curves. For 18S rRNA, we used 15 cycles of amplification; for MASH I we used 33 cycles of amplification [Fig. 4(D)] for analysis of samples from different animals. In retrospect, it appears that the number of cycles of amplification selected for MASH I may have actually led to an under representation of the effect of VAD on the expression of this gene, because, as can be seen, the difference between VAD and VAS product yield is even greater at 35–36 cycles of amplification, and product yield is still within the linear range of amplification.

Effect of VAD on MASH I mRNA Levels—Quantitative RT-PCR was carried out to determine the effect of VAD on the expression of MASH I mRNA levels in olfactory tissue. MASH I levels were increased approximately two- to threefold in VAD olfactory tissue relative to levels in VAS samples. This difference was statistically significant (Table II$p < .01$, Mann-Whitney Rank Sum Test). As expected, the levels of the internal control gene, 18S rRNA, were unaffected by VAD (VAD samples were 97–101% of control levels, Table II$p = 0.31$, Mann-Whitney Rank Sum test).

DISCUSSION

Current evidence suggests that cells in the basal region of the OE give rise to mature neurons through a process involving multiple steps, beginning with clonal expansion of a precursor cell population, followed by differentiation of the precursor cells into immature and finally, postmitotic, mature neuron phenotypes. Keratin$^+$ basal cells are thought to give rise to the immediate neuronal precursor in this system. The neuronal precursor putatively divides and differentiates into two N-CAM$^+$ (neural cell adhesion molecule) neurons, which, in turn, differentiate into cells that express the neuron-specific marker protein, GAP-43, and finally, into fully specialized olfactory receptor neurons that are positive for the cytoplasmic marker protein, OMP (Calof and Chikaraishi, 1989; Verhaagen et al., 1989; Mackay-Sim and Chuah, 2000). This model is supported by results obtained from studies showing OE recovery after injury. When postnatal rats are transiently exposed to methyl bromide, much of the OE is destroyed. Within hours, after removal to normal air conditions, basal cells in the damaged OE begin to proliferate. Following a build-up of the population of progenitor cells, sequential waves of differentiated immature neurons and then, mature neurons appear over the course of several weeks (Schwob et al., 1995). This step-by-step process of

epithelial regeneration over time indicates that (1) proliferation and differentiation occur as distinct events with mechanisms in place to promote regulated progression through sequential phases of development, and (2) loss of differentiated neurons from the OE signals neuronal precursors to repopulate the OE. It has been suggested that differentiated olfactory neurons keep progenitor cell proliferation in check by signaling progenitor cells to proliferate only as the supply of mature olfactory neurons decreases (Calof et al., 1998; Farbman et al., 1999).

We have found that VAD leads to decreased expression of OMP mRNA in OE from mature rats and increased expression of PCNA protein. Cell density is unaffected by VAD, but the distribution of cells within the OE is altered in VAD tissue. There are more cells in the basal region of VAD OE, and relatively high levels of hyperplasia are displayed in some areas of the OE. Reactivity with the PCNA antibody indicates that proliferation is increased over control levels in the basal region of VAD OE. Previous work in our laboratory (to be published elsewhere) has indicated that VAD is not specifically affecting OMP mRNA expression, because adenylate cyclase mRNA (also a marker for mature olfactory neurons) levels are also decreased in VAD OE. Together, our results suggest that neuron replacement is substantially reduced and proliferation of cells in the basal region of the OE is substantially increased in VAD OE.

We determined there was an average of 9 $PCNA^+$ cell profiles/mm OE in the basal region of vitamin A-sufficient animals. This measurement is comparable to published values determined using BrdU as an alternative marker of cell proliferation. The mean $BrdU^+$ cell profile densities of vitamin A-sufficient rats of similar age (181 days) was 10 cell profiles/mm OE (Weiler and Farbman, 1997). The densities of $PCNA^+$ cell profiles in the OE of vitamin A-deprived animals were greatly increased in the study reported here. The number of $PCNA^+$ cell profiles per mm OE was an average of fivefold higher in VAD animals than it was in the OE of age-matched, vitamin A-sufficient control rats. This relative increase in the number of proliferative cells in VAD OE is particularly noteworthy because cell proliferation in the OE normally declines with rat age (Weiler and Farbman, 1997). To put this in perspective, the densities of $PCNA^+$ cell profiles that we observed in vitamin A-deprived OE are more in line with the mean densities of $BrdU^+$ cell profiles that have been observed in OE from vitamin A-sufficient rats that are barely beyond the stage of weaning (postnatal day 21; Weiler and Farbman, 1997). These data support the conclusion that cell proliferation is upregulated in postnatal, vitamin A-deficient OE.

In 1925, Wolbach and Howe stated in their classic paper describing the histopathology of vitamin A-deficient rats, “Loss of power to smell was a late but constant symptom … Each animal was fed and watched and after loss of smell occurred, the food was actually placed in its mouth until the ration was consumed” (Wolbach and Howe, 1925). Despite the purported deficiency in olfactory acuity, the authors reported that the OE was “always intact except for instances of inflammatory changes and invasion by growth of adjacent keratinizing epithelium.” They went on to say there were no visible effects of VAD on cell density in rat epithelia and commented that if anything, cell densities appeared to be greater in VAD tissue, with signs of “neoplasia” evident in some tissue sections. Relying on visual examination of stained tissue sections as their only tool, they stated simply and with amazing prescience “It is also evident that factors essential to epithelial proliferation are abundantly present in advanced fat-soluble A vitaminosis. Function, possibly to be expressed as maintenance of differentiation is interfered with” (Wolbach and Howe, 1925). The possibility that olfaction might be adversely affected by VAD was addressed again in 1951 by Le Magnen and Rapaport, who reported that dietary deficiency in vitamin A caused anosmia in rats (Le Magnen and Rapaport, 1951). In 1985, Biesalski et al. questioned whether the anosmia reported in VAD rats might be due to “… a degeneration of the

respiratory epithelia or an alteration of the sensory cells." The latter authors examined electron micrographs of olfactory tissue from VAD guinea pigs and reported a degeneration of the cilia in the vitamin deprived group. They were unable to conclude, however, whether the respiratory or "gustatory" epithelium was more affected by the vitamin A deficiency (Biesalski et al., 1985).

Our data confirm the predictions of Wolbach and Howe (1925) and suggest that VAD interferes with olfactory acuity because VAD OE has fewer mature neurons. This conclusion offers an explanation for the results of Biesalski et al. (1985) because a loss of mature neurons would surely result in a loss of sensory cilia. We propose that retinoic acid influences the development of olfactory neurons by exerting an effect(s) at key steps that prompt cells to shut down mitosis and turn on gene expression programs that will promote neuron differentiation. Our data suggest that neuron replacement may be thwarted in VAD OE because proliferating progenitor cells are not provided with appropriate signals to proceed to maturity.

Recent studies indicate that stage- and cell-specific transcription factors are expressed in differentiating olfactory neuronal progenitor cells (Mackay-Sim and Chuah, 2000). MASH I, a mammalian homolog of the *Drosophila* neural determination genes, achaetescute, is one of these factors. MASH I is a basic helix-loop-helix (bHLH) protein that exhibits transient expression in proliferating, but not overtly differentiating pro-neural cells, and that is required for the development of many different neural lineages (Lo et al., 1991; Kageyama et al., 1997). It has been immunolocalized to postnatal mice olfactory neural progenitor cells (Gordon et al., 1995). Mice mutant for the gene Mash 1 display severe neuronal losses in the olfactory epithelium, indicating its importance for the development of neurons in this system (Guillemot et al., 1993). MASH I activity is at least partially regulated by the presence of other bHLH proteins (Kageyama et al., 1997; Cau et al., 2000). Hes1 has been shown to inhibit cell differentiation by inhibiting MASH I activity. Hes6 has been observed to suppress the activity of Hes1, thus alleviating inhibition on MASH I and promoting cell differentiation (Bae et al., 2000). Thus, MASH I expression appears to identify a subset of proliferative pro-neural cells that are poised to proceed to maturity given the availability of appropriate signaling molecules to downregulate mitosis and upregulate differentiation.

Retinoic acid has been shown to be required for neurogenesis. Expression of some bHLH proteins is induced in response to retinoic acid, including MASH I and HES I (Johnson et al., 1992; Wakabayashi et al., 2000), although precisely which genes are affected by retinoic acid and at what times retinoic acid is effective during the developmental program is not known. We tested effects of VAD on the expression of MASH I mRNA levels and found them to be significantly increased over control levels. We do not believe that mRNA expression was induced, because retinoic acid is not present in the VAD olfactory tissue and other inducing agents of MASH I have not been identified. Rather, we interpret the increased expression levels to be indicative of an increase in the numbers of MASH I-positive pro-neural cells in VAD olfactory tissue. Expression of MASH I has been described in proliferative pro-neural cells and has been specifically noted to be present in a subset of basal OE cells (Gordon et al., 1995). An increase in a subpopulation of MASH I-positive pro-neural cells is thus, consistent with these reports and with our observations of increased proliferation of basal cells in VAD OE. We suggest that a lack of retinoic acid inhibits maturation of olfactory neurons because a necessary transcription factor is not synthesized or activated at a stage involving or subsequent to the expression of MASH I.

Olfactory neurons normally die by apoptosis (Simmons et al., 1981; Magrassi and Graziadei, 1995), and it has been proposed that for every neuron lost, a new one is born in the postnatal OE (Gordon et al., 1995; Farbman et al., 1999). This notion is supported by the observation

that surgical ablation of the olfactory bulb leads to a concomitant loss of neurons and upregulation of basal cell proliferation within hours of the insult (Costanzo and Graziadei, 1983; Carr and Farbman, 1993; Calof et al., 1998). Thus, an alternative explanation for the loss of neurons and coincident induction of cell proliferation we observe in retinoid deficient OE could be that vitamin A derivatives exert effects at a key step(s) in the apoptotic pathway, such that neurons and/or postmitotic, post-MASH I^+ differentiated cells are precociously targeted for death in retinoic acid depleted tissue, thus preventing reestablishment of the mature olfactory neuron population. A death-induced block in the replacement of mature neurons could induce basal precursor cells to continue to replicate and progress to maturity in a futile effort to reestablish the lost population of functional neurons. We are currently carrying out experiments to determine whether vitamin A status is affecting neurogenesis and/or apoptosis in the postnatal OE.

Acknowledgments

Contract grant sponsor: NIH; contract grant numbers: S-06-GM-08092 and 5 KO2 DC00180-02.

We thank Anne Ilvarsonn, Obaydah Ahmad, and W. Bradford Smith for technical assistance.

References

Anchan RM, Drake DP, Haines CF, Gerwe EA, LaMantia AS. Disruption of local retinoid-mediated gene expression accompanies abnormal development in the mammalian olfactory pathway. J Comp Neurol. 1997; 379:171–184. [PubMed: 9050783]

Bae S, Bessho Y, Hojo M, Kageyama R. The bHLH gene Hes6, an inhibitor of Hes1, promotes neuronal differentiation. Development. 2000; 127:2933–2943. [PubMed: 10851137]

Bain G, Ray WJ, Yao M, Gottlieb DI. Retinoic acid promotes neural and represses mesodermal gene expression in mouse embryonic stem cells in culture. Biochem Biophys Res Commun. 1996; 223:691–694. [PubMed: 8687458]

Balboni GC, Zonefrati R, Repice F, Barni T, Vannelli GB. Immunohistochemical detection of EGF and NGF receptors in human olfactory epithelium. Boll Soc Ital Biol Sper. 1991; 67:901–906. [PubMed: 1668217]

Biesalski HK, Wellner U, Stofft E, Bassler KH. Vitamin A deficiency and sensory function. Acta Vitaminol Enzymol. 1985; 7(Suppl):45–54. [PubMed: 3916045]

Calof AL, Chikaraishi DM. Analysis of neurogenesis in a mammalian neuroepithelium: proliferation and differentiation of an olfactory neuron precursor in vitro. Neuron. 1989; 3:115–127. [PubMed: 2482777]

Calof AL, Rim PC, Askins KJ, Mumm JS, Gordon MK, Iannuzzelli P, Shou J. Factors regulating neurogenesis and programmed cell death in mouse olfactory epithelium. Ann NY Acad Sci. 1998; 855:226–229. [PubMed: 9929610]

Carr VM, Farbman AI. The dynamics of cell death in the olfactory epithelium. Exp Neurol. 1993; 124:308–314. [PubMed: 8287929]

Cau E, Gradwohl G, Casarosa S, Kageyama R, Guillemot F. Hes genes regulate sequential stages of neurogenesis in the olfactory epithelium. Development. 2000; 127:2323–2332. [PubMed: 10804175]

Costanzo RM, Graziadei PP. A quantitative analysis of changes in the olfactory epithelium following bulbectomy in hamster. J Comp Neurol. 1983; 215:370–381. [PubMed: 6863590]

Dickman ED, Thaller C, Smith SM. Temporally-regulated retinoic acid depletion produces specific neural crest, ocular and nervous system defects. Development. 1997; 124:3111–3121. [PubMed: 9272952]

Drager UC, Wagner E, McCaffery P. Aldehyde dehydrogenases in the generation of retinoic acid in the developing vertebrate: a central role of the eye. J Nutr. 1998; 128:463S–466S. [PubMed: 9478049]

Farbman AI, Buchholz JA, Suzuki Y, Coines A, Speert D. A molecular basis of cell death in olfactory epithelium. J Comp Neurol. 1999; 414:306–314. [PubMed: 10516598]

Gordon MK, Mumm JS, Davis RA, Holcomb JD, Calof AL. Dynamics of MASH1 expression in vitro and in vivo suggest a non-stem cell site of MASH1 action in the olfactory receptor neuron lineage. Mol Cell Neurosci. 1995; 6:363–379. [PubMed: 8846005]

Graziadei PP, Graziadei GA. Neurogenesis and neuron regeneration in the olfactory system of mammals. I. Morphological aspects of differentiation and structural organization of the olfactory sensory neurons. J Neurocytol. 1979; 8:1–18. [PubMed: 438867]

Guillemot F, Lo LC, Johnson JE, Auerbach A, Anderson DJ, Joyner AL. Mammalian achaetescute homolog 1 is required for the early development of olfactory and autonomic neurons. Cell. 1993; 75:463–476. [PubMed: 8221886]

Hoover F, Gundersen TE, Ulven SM, Michaille JJ, Blanchet S, Blomhoff R, Glover JC. Quantitative assessment of retinoid signaling pathways in the developing eye and retina of the chicken embryo. J Comp Neurol. 2001; 436:324–335. [PubMed: 11438933]

Johnson JE, Zimmerman K, Saito T, Anderson DJ. Induction and repression of mammalian achaetescute homologue (MASH) gene expression during neuronal differentiation of P19 embryonal carcinoma cells. Development. 1992; 114:75–87. [PubMed: 1576967]

Kageyama R, Ishibashi M, Takebayashi K, Tomita K. bHLH transcription factors and mammalian neuronal differentiation. Int J Biochem Cell Biol. 1997; 29:1389–1399. [PubMed: 9570134]

Kelley MW, Turner JK, Reh TA. Retinoic acid promotes differentiation of photoreceptors in vitro. Development. 1994; 120:2091–2102. [PubMed: 7925013]

Kelley MW, Williams RC, Turner JK, Creech-Kraft JM, Reh TA. Retinoic acid promotes rod photoreceptor differentiation in rat retina in vivo. Neuroreport. 1999; 10:2389–2394. [PubMed: 10439469]

LaMantia AS, Colbert MC, Linney E. Retinoic acid induction and regional differentiation prefigure olfactory pathway formation in the mammalian forebrain. Neuron. 1993; 10:1035–1048. [PubMed: 8318228]

Le Magnen J, Rapaport A. Essai de determination du role de la vitamin A dans le mecanisme de l'olfaction chez le rat blanc. CR Soc Biol. 1951; 145:800–803.

Lo LC, Johnson JE, Wuenschell CW, Saito T, Anderson DJ. Mammalian achaetescute homolog 1 is transiently expressed by spatially restricted subsets of early neuroepithelial and neural crest cells. Genes Dev. 1991; 5:1524–1537. [PubMed: 1909283]

Mackay-Sim A, Chuah MI. Neurotrophic factors in the primary olfactory pathway. Prog Neurobiol. 2000; 62:527–559. [PubMed: 10869782]

Magrassi L, Graziadei PP. Cell death in the olfactory epithelium. Anat Embryol (Berl). 1995; 192:77–87. [PubMed: 7486003]

Murray RC, Calof AL. Neuronal regeneration: lessons from the olfactory system. Semin Cell Dev Biol. 1999; 10:421–431. [PubMed: 10497099]

Niederreither K, Vermot J, Schuhbaur B, Chambon P, Dolle P. Retinoic acid synthesis and hindbrain patterning in the mouse embryo. Development. 2000; 127:75–85. [PubMed: 10654602]

Schwob JE, Youngentob SL, Mezza RC. Reconstitution of the rat olfactory epithelium after methyl bromide-induced lesion. J Comp Neurol. 1995; 359:15–37. [PubMed: 8557844]

Simmons PA, Rafols JA, Getchell TV. Ultrastructural changes in olfactory receptor neurons following olfactory nerve section. J Comp Neurol. 1981; 197:237–257. [PubMed: 7276234]

Smith D, Wagner E, Koul O, McCaffery P, Drager UC. Retinoic acid synthesis for the developing telencephalon. Cereb Cortex. 2001; 11:894–905. [PubMed: 11549612]

Smith JE. Preparation of vitamin A-deficient rats and mice. Methods Enzymol. 1990; 190:229–236. [PubMed: 2087174]

Verhaagen J, Oestreicher AB, Gispen WH, Margolis FL. The expression of the growth associated protein B50/GAP43 in the olfactory system of neonatal and adult rats. J Neurosci. 1989; 9:683–691. [PubMed: 2918383]

Wakabayashi N, Kageyama R, Habu T, Doi T, Morita T, Nozaki M, Yamamoto M, Nishimune Y. A novel *cis*-acting element regulates HES-1 gene expression in P19 embryonal carcinoma cells treated with retinoic acid. J Biochem (Tokyo). 2000; 128:1087–1095. [PubMed: 11098153]

Wang AM, Doyle MV, Mark DF. Quantitation of mRNA by the polymerase chain reaction. Proc Natl Acad Sci USA. 1989; 86:9717–9721. [PubMed: 2481313]

Weiler E, Farbman AI. Proliferation in the rat olfactory epithelium: age-dependent changes. J Neurosci. 1997; 17:3610–3622. [PubMed: 9133384]

White JC, Highland M, Kaiser M, Clagett-Dame M. Vitamin A deficiency results in the dose-dependent acquisition of anterior character and shortening of the caudal hindbrain of the rat embryo. Dev Biol. 2000; 220:263–284. [PubMed: 10753515]

Wilkinson, M. Purification of RNA. In: Brown, TA., editor. Essential molecular biology: a practical approach. Oxford: IRL Press; 1991. p. 69-87.

Wolbach SB, Howe PR. Tissue changes following deprivation of fat-soluble A vitamin. J Exp Med. 1925; 62:753–777. [PubMed: 19869087]

Young JT. Histopathologic examination of the rat nasal cavity. Fundam Appl Toxicol. 1981; 1:309–312. [PubMed: 6764423]

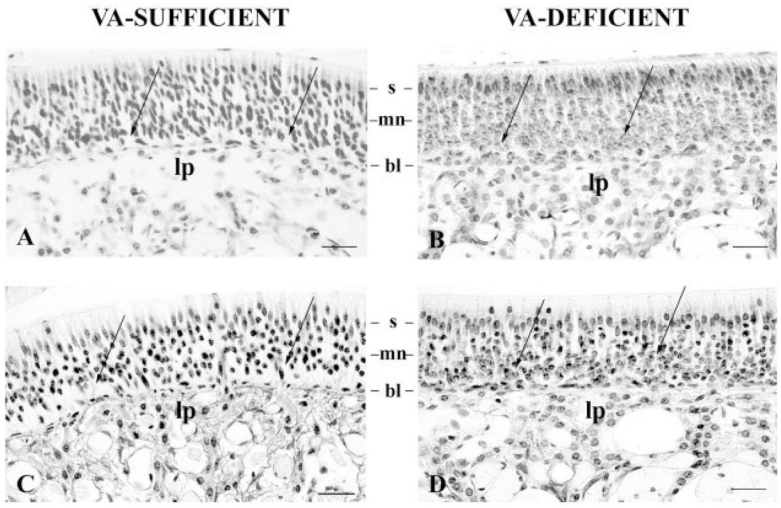

Figure 1.

Comparison of VAS and VAD OE from postnatal rats. Shown are images from coronal sections of *regio olfactoria* from VA-sufficient (A, animal N3 and C, animal N4) and VA-deficient (B, animal D5 and D, animal D24) rats. Note there are more cell bodies along the basal lamina of the VA-deficient OE (arrows) than there are along the basal lamina of the VA-sufficient OE. Note there is also a greater density of cell nuclei in the layers immediately above the basal lamina of VA-deficient OE than there are in corresponding regions of the VA-sufficient tissues [compare (B) and (D) with (A) and (C)]. Scale bars in the lower right of each plate represent 20 μm. Key to figure labels: s, sustentacular cell body layer; mn, mature neuron layer; bl, basal lamina; lp, *lamina propria*.

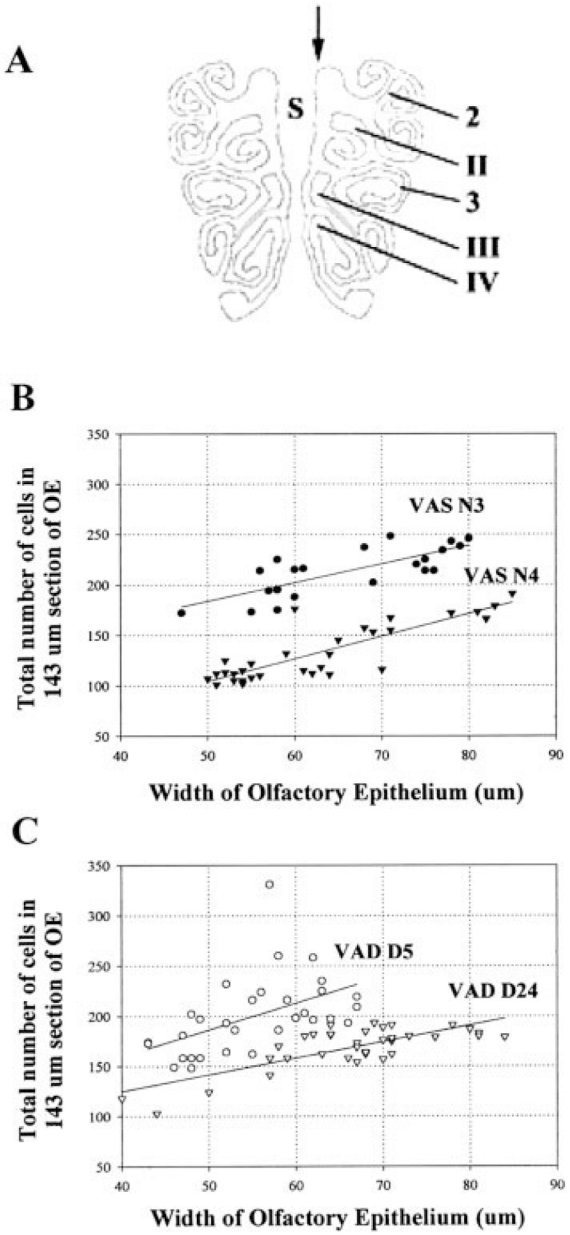

Figure 2.

Comparison of total cell number in VAS and VAD OE. (A) Computer-generated map of a coronal section of *regio olfactoria* from a vitamin A-sufficient (N4) rat. Cell nuclei were counted in the OE lining one side of the nasal septum (specified by the arrow). Key to figure labels: s, nasal septum; 2 and 3, ectoturbinates; II, III, and IV, endoturbinates. (B, C) Toluidine-blue stained nuclei in the OE lining one side of the nasal septum of VAS and VAD rats were counted and tabulated using a BIOQUANT computerized image analysis system as described in the text. Data from two vitamin A-sufficient rats (VAS animal N3 and VAS animal N4) are shown in (B), and data from two vitamin A-deficient rats (VAD animal D5 and VAD animal D24) are shown in (C). Key to symbols: ● VAS rat N3; ▼ VAS rat N4; ○ VAD rat D5; ▽ VAD rat D24.

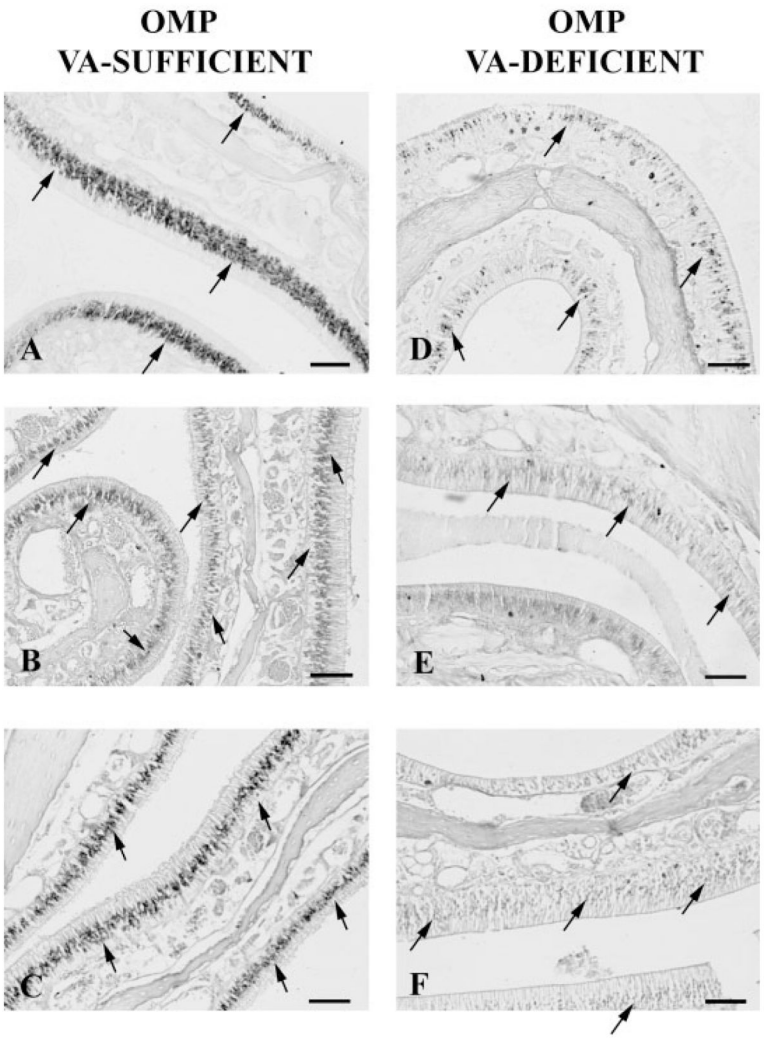

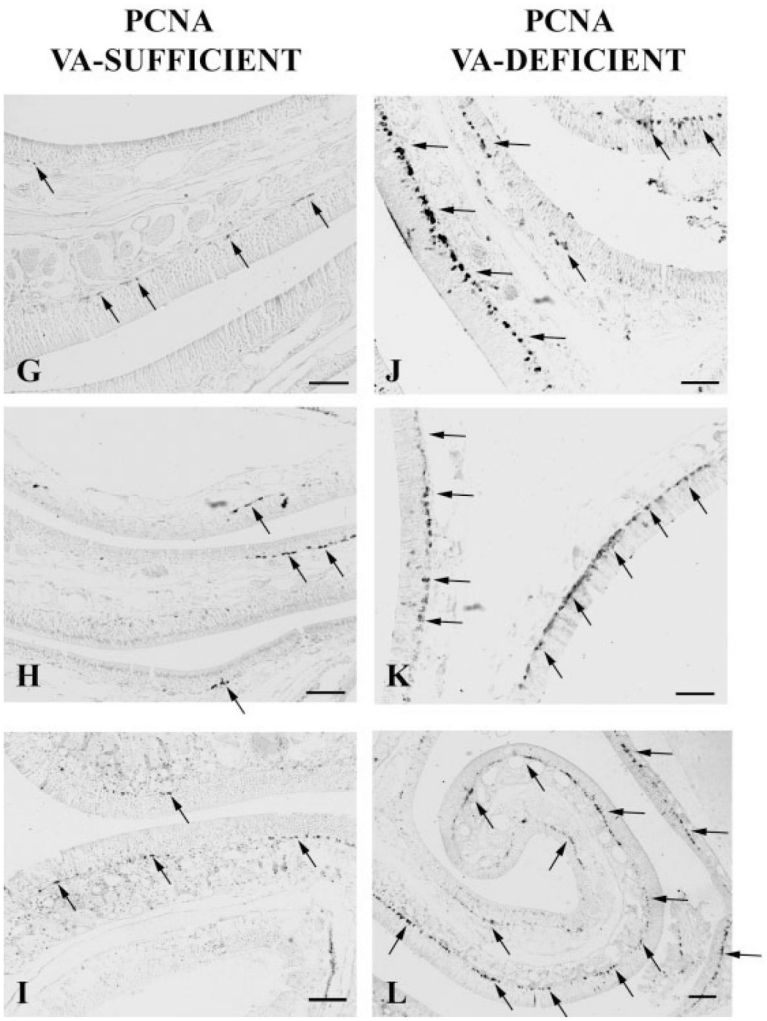

Figure 3.

Comparison of the expression of OMP mRNA and PCNA protein in VAS and VAD OE. Coronal sections from similar regions of the *regio olfactoria* from three different VA-sufficient rats [(A) and (G), animal N2; (B) and (H), animal N3; and (C) and (I), animal N4] and three different VA-deficient rats [(D) and (J), animal D5; (E) and (K), animal D14; and (F) and (L), animal D24] were reacted with a digoxigenin-labeled antisense OMP riboprobe (A–F) or with an antibody directed against PCNA (G–L). Tissues were fixed in paraformaldehyde, processed, and embedded in paraffin. Color development was with nitroblue tetrazolium (NBT)/5-bromo-4-chloro-3-indolyl phosphate (BCIP) for sections reacted with the riboprobe [note stained cell bodies designated by arrows in the central region of the OE, (A–F)] and with DAB for sections reacted with the antibody [note stained cell bodies designated by arrows along the basal lamina of the OE, Fig. (G–L)]. Note the larger number of OMP^+ cell bodies in the VA-sufficient tissue sections as compared to the VA-deficient tissue sections [(A), (B), and (C) compared with (D), (E), and (F)]. Note the larger number of $PCNA^+$ cell bodies that lie along the basal lamina of the VA-deficient OE as compared with the VA-sufficient OE [(J), (K), and (L) compared with (G), (H), and (I)]. Scale bars in the lower right of each plate represent 50 μm.

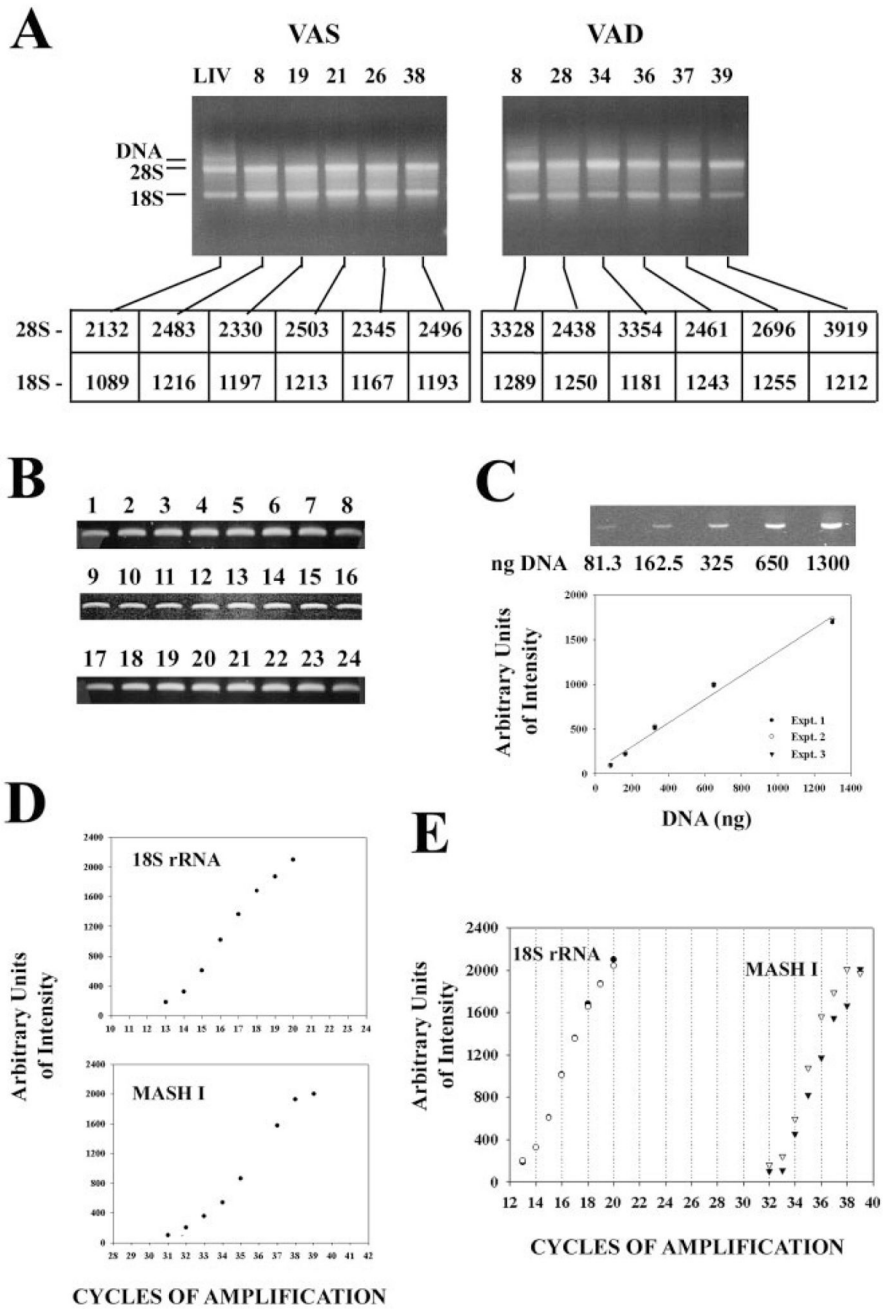

Figure 4.

VA deficiency leads to increased expression of MASH I mRNA levels in postnatal olfactory tissue. (A) Total RNA (0.5 μg) isolated from the liver (LIV) of a VAS rat or the OE of VAS rats 8, 19, 21, 26, and 38 and VAD rats 8, 28, 34, 36, 37, and 39 was separated on an agarose gel and stained with ethidium bromide. All RNA samples, except the LIV sample, were treated with DNAse I. The location of contaminating DNA bands and the 28S rRNA and 18S rRNA bands is indicated. The intensities of the 28S and 18S rRNA bands were determined using a BIO-RAD Gel Doc 1000 Imaging System with Quantity One Software. The intensities of bands in each corresponding RNA sample are shown in the table beneath the images. (B) Twenty-four identical RT-PCR were prepared and incubated in the 24 wells

of a PE 2400 Thermocycler. The reaction products (10 μL) were separated on three agarose gels (wells in one gel were loaded with samples 1– 8; wells in the second gel were loaded with samples 9 –16; and wells in the third gel were loaded with samples 17–24) and stained with SYBR Gold. The single product that was observed in each sample is shown here (the size of the band was approximately 300 bp relative to 100 bp ladder, data not shown). (C) The remaining 90 μL of each of the samples shown in (B) were pooled, and the DNA concentration was determined by spectrophotometry. Increasing amounts of DNA (81.3–1300 ng DNA, as indicated) in the pooled reaction mix were separated on three different agarose gels (Experiments 1, 2, and 3) and stained with SYBR Gold. The intensity of the stained single band in each lane was measured using BIO-RAD Gel Doc 1000 Imaging System with Quantity One Software. Band intensities were plotted against ng DNA, and the best fit line was determined by least squares linear regression. As can be seen, the data from the three experiments overlap, and band intensities show a positive correlation with sample DNA content ($Y = 1.3 \times + 40.7$; $r^2 = 0.99$). (D) RT-PCR reactions were prepared in separate tubes using primers for either 18S rRNA or MASH I and DNAse I-treated total RNA from the olfactory tissue of one VAS animal and were carried out for increasing cycles of amplification to determine product yield curves. Reaction products obtained after increasing cycles of amplification were separated on an agarose gel and stained with Sybr Green I. Band intensities were determined using the Gel-Doc image analysis system described above, and the product yield curves for 18S rRNA (upper curve) and MASH I (lower curve) were plotted using Sigma Plot, ver. 8.0. Note that 18S rRNA is first detected by this method after 13 cycles of amplification and begins to plateau after 20 cycles of amplification; MASH I is first detected after 31 cycles of amplification and begins to plateau after 38 cycles of amplification. (E) RT-PCR reactions were prepared using primers for either 18S rRNA or MASH I and DNAse I-treated total RNA from the olfactory tissue of one VAS and one VAD animal. Amplification of the reactions and analysis of band intensities was as described in (D), above. Reactions were carried out in separate tubes, but the results are plotted on a single graph for ease of comparison of the results. Note that the intensities of the 18S rRNA reaction products overlap for all data points (● VAS RNA, ○ VAD RNA, cycles 13–20). Note that in the linear range of amplification, the intensities of the MASH I reaction products are greater for the VAD RNA (▽) for a given number of cycles of amplification than they are for the VAS RNA (▼) (cycles 32–38).

J Neurobiol. Author manuscript; available in PMC 2011 November 23.

Table 1

Characteristics of Rats Maintained on the Vitamin A-Sufficient (VAS) or Vitamin A-Deficient (VAD) Diets in This Study

Group-Rat ID	Age at Sac[a]	Initial Wt[b]	Peak Wt	Wt at Sac	Indicators of VAD[c]
VAS-N2	162	80	—	329	None
VAS-N3	185	84	—	327	None
VAS-N4	185	98	—	407	None
VAD-D5	182	90	385	300	1, 2, 3,
VAD-D14	182	82	330	210	1, 2, 3
VAD-D24	178	90	373	266	1, 2, 3, 4
VAS-N7	166	88	—	306	None
VAS-N8	166	78	—	346	None
VAS-N19	166	80	—	361	None
VAS-N21	166	82	—	313	None
VAS-N26	166	94	—	357	None
VAS-N38	175	80	—	347	None
VAD-D8	165	76	298	217	1, 2, 3, 4
VAD-D28	175	92	383	290	1, 2, 4
VAD-D34	165	82	370	272	1, 3, 4
VAD-D36	165	94	424	312	1, 2, 3, 4
VAD-D37	165	76	382	261	1, 3, 4
VAD-D39	165	78	347	255	1, 2, 3, 4

[a] Sac = sacrifice.

[b] Wt = animal weight in g.

[c] 1, 20 –30% decline in weight; 2, white lower incisors; 3, alopecia; 4, ataxia.

Table 2

Effect of Vitamin A Deficiency on Expression of MASH I in Olfactory Tissue From Postnatal Rats

	18S rRNA		MASH I	
ID	**Band Intensity**[a]	**Percent of Control**	**Band Intensity**	**Percent of Control**
Control (*N* = 5)				
Mean ± S.D.	795 ± 25	100	555 ± 8	100
D28	799	101	940	169
D34	781	98	943	170
D36	776	98	1078	194
D37	771	97	940	169
D39	777	98	1969	355

[a]Band Intensity is an arbitrary measure of signal strength assigned by the BioRad Gel Doc 1000 Imaging system.